AIRPORT ADVISORY BOARD AGENDA

AIRPORT MEETING ROOM | WEDNESDAY, JULY 21, 2021 | 7:00 AM

1. Call to Order
2. Approval of the Minutes of June 16, 2021
3. Airport Manager Update
4. Other
   A. Airfield Matters
   B. Proposed Solar Array
   C. Fuel System Hose
   D. Federal Funding
   E. Capital Improvement Plan
   F. Runway Extension
   G. Open House
5. Next Meeting Date: August 18, 2021
6. Adjournment

GLARE STUDY

USS Fair Park Solar LLC

Rice County, Minnesota

JUNE 22, 2021

PREPARED FOR:

PREPARED BY:

Glare Study for

USS Fair Park Solar LLC

Rice County, Minnesota

Prepared for:
USS Fair Park Solar LLC
100 N. 6th Street, Suite 410B Center Dr.
Minneapolis, MN 55403

Prepared by:
Westwood Professional Services
12701 Whitewater Drive, Suite 300
Minnetonka, MN, 55343

Project Number: 0027180.58
Date: June 22, 2021

TABLE OF CONTENTS

TABLES

FIGURES

EXHIBITS

APPENDICES

EXECUTIVE SUMMARY

Westwood Professional Services (Westwood) completed a glint and glare study for the proposed USS Fair Park Solar LLC (Project) located in Rice County, Minnesota. This analysis used an average six-foot array structure height for all arrays. The analyses were modeled with a 10-degree solar panel resting angle. Four flight paths for the Faribault Airport were assessed for this study. No residences or routes were identified as Observation Points (OPs).

With a six-foot array height and 10-degree rest angle, the model reported no glare from the proposed array to the four flight paths assessed and that the assessment passed the Forge Solar FAA policy adherence. The findings are detailed in **Appendix A**.

1.0 INTRODUCTION

Westwood Professional Services, Inc., (Westwood) was contracted by US Solar to prepare a glare study of four flight paths to the Faribault Airport for the proposed Project. The Project is located west of Interstate-35 northwest of the intersection of 183rd St. West and Parkland Drive northwest of Faribault, Rice County, Minnesota. It covers a portion of Section 23 in T110N R21W (**Exhibit 1**).

USS Fair Park Solar LLC will consist of a series of photovoltaic (PV) modules fixed to single axis solar trackers. Panels will be placed with project infrastructure within an approximately 8.1-acre Project Area (**Exhibit 2**).

Specifically, this study answers the following questions:

1. Will glint or glare from the PV modules be visible to pilots that utilize these flight paths?
2. If glint or glare is visible, what is it comparable to?

1.1 General Discussion of Reflection

With growing numbers of solar energy facilities being proposed and installed throughout the United States, the potential impact of glint and glare from PV modules and other types of solar collection systems is receiving increased attention as a potential nuisance to neighboring residential properties or potential hazard or distraction for vehicle drivers, pilots and air-traffic control personnel at nearby airports.

A common misconception about solar PV modules is that they inherently cause or create a lot of glare, posing a nuisance to neighbors and a safety risk for pilots. While in certain situations the glass surfaces of solar PV systems can produce glint (a momentary flash of bright light) and glare (a reflection of bright light for a longer duration), light absorption, rather than reflection, is central to the function of a solar PV panel. PV modules absorb solar radiation that is converted to electricity. Solar PV modules are constructed from high transmission, low iron glass and are covered with anti-reflective (AR) coatings. Modern PV modules reflect as little as two percent of incoming sunlight, about the same as water and less than soil or even wood shingles (Sandia 2014).

1.1.1 Reflection Type from Solar Modules

Smooth surfaces such as glass and still water exhibit specular reflection. Specular reflection is when light hits the surface at one angle and is reflected in another direction, like a mirror. Specular reflection can be contrasted with diffuse reflection, which occurs when light reflects off microscopically rough surfaces and scatters. Diffuse reflection is what happens when light hits virtually everything in our field of vision**.** The difference between the two types of reflections are illustrated in **Figure 1**. Since solar modules are flat and have a relatively smooth surface, most of the light reflected is specular, meaning that incident light from a specific direction is reradiated in a different direction.

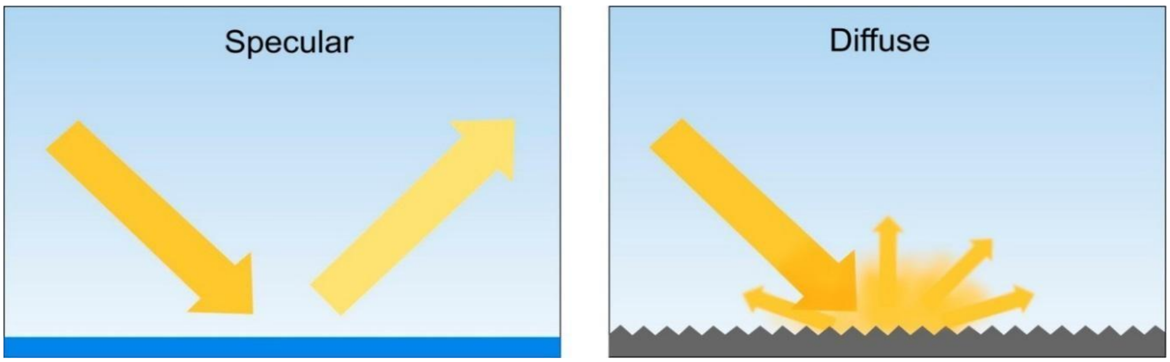

Figure 1: Specular and Diffuse Reflections

When the sun is reflected on a smooth surface, it can result in glint or glare for those who are on the receiving angle. In both cases, the light reflected is diminished by having first hit the substrate that reflected it–unless that surface is a perfect mirror. When the sun is the original source of the light reflected off a reflective surface, the time and position at which glare or glint might occur depends on the original position of the sun in the sky in relation to the location of the viewer.

1.1.2 Relative Reflectance of Solar Modules Compared to Other Surfaces

Solar modules are designed to absorb light, and accordingly reflect only a small amount of the sunlight that falls on them compared to most other everyday objects. Most notably, solar modules reflect significantly less light than flat water or standard window glass. In fact, glass, one of the uppermost and important components of a solar panel, reflects only a small portion of the light that falls on it–about 2-4 percent, depending on whether it received an anti-reflective coating (ARC). To increase solar panel efficiency and power output, most of the solar PV modules in use today are treated with an ARC. An example of how antireflective technology can increase light transmission in glass and reduce overall reflection is provided in **Figure 2**. Standard low-iron glass reflects approximately 8 percent of light, whereas AR-glass modules reflect a total of approximately 2-3 percent of the light.

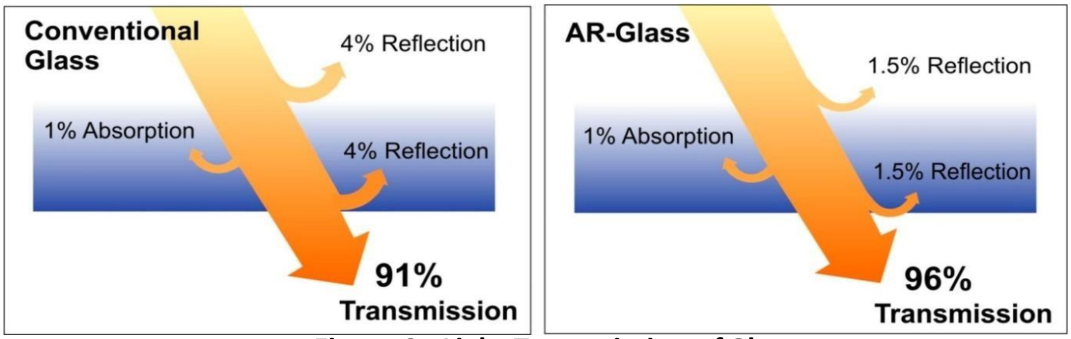

Figure 2: Light Transmission of Glass

Several studies have been conducted which have measured the intensity of reflections from PV solar modules with respect to other naturally occurring and manmade surfaces. The results of the studies show that reflections of the sun from solar modules are possible; however, the reflections produced will be of intensity similar to, or less than, those produced from still water and significantly less than reflections from glass and steel. The reflectivity of solar modules relative to other natural or manmade surfaces are provided in **Figures 3** and **4**.

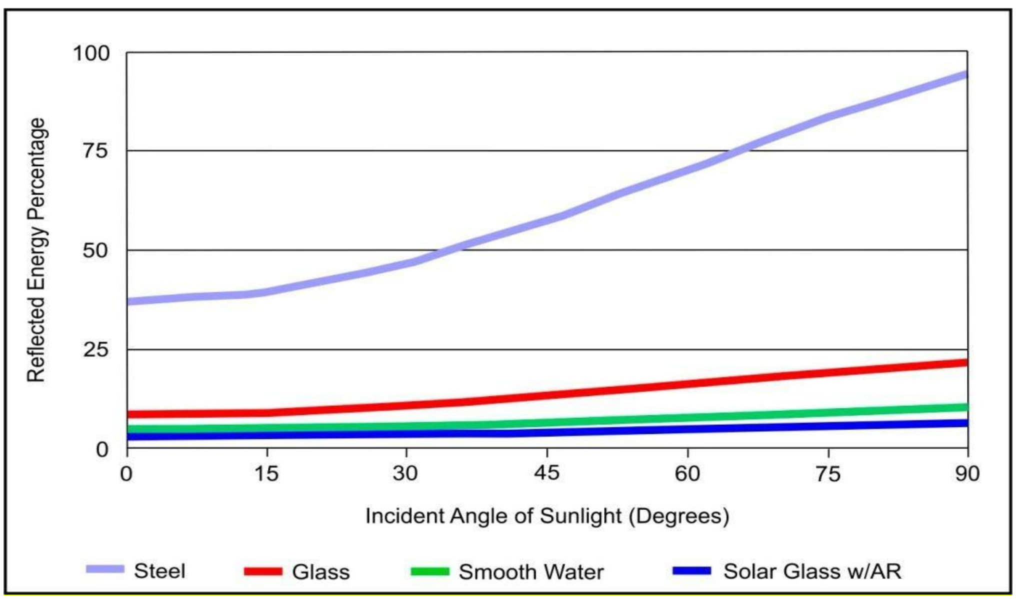

Figure 3: Analysis of Typical Material Reflectivity with Sunlight Angle (Source: Capital Solar Farm Visual Impact Assessment, 2010)

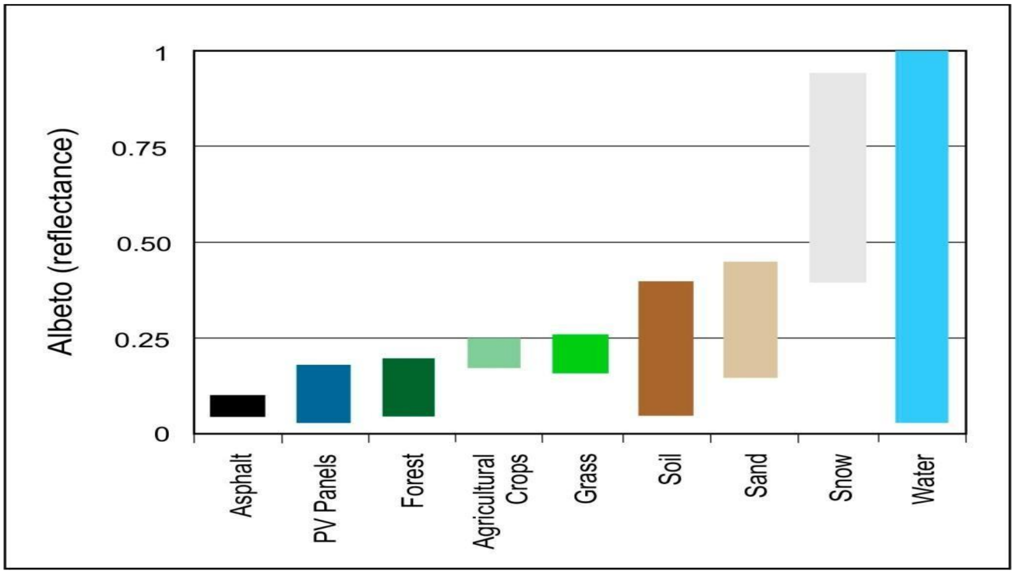

Figure 4: Albedo for Various Common Surfaces (Source: Capital Solar Farm Visual Impact Assessment, 2010)

One measure of reflectivity is albedo, the ratio of solar radiation across the visible and invisible light spectrum reflected by a surface. Albedo varies between 0, a surface that reflects no light, and 1, a mirror-like surface that reflects all incoming light. Solar PV modules with a single ARC have a reflectivity of between 0.03 and 0.18. Common sand has an albedo between 0.15 and 0.45 and agricultural vegetation has an albedo between 0.18 and 0.25. This diffuse reflectivity measure is consistent with the intent of solar PV modules to absorb most of the solar energy for conversion to electricity.

1.2 Important Considerations

When reflection occurs, unless it is directed toward, and seen by, an abutting property (hereafter, receptor, or observer), glint will not pose a concern. This was determined after modelling the potential for glint and glare with surface characteristics from typical PV modules with the GlareGauge analysis tool.

Before considering the mathematics of sunlight reflectivity, it is important to understand several fundamental limitations concerning the extent to which glare might be visible to nearby air-traffic control facilities.

First, for glare to appear, the observer must be able to see the tops of the PV modules. For this to occur, at a minimum, the receptor would need to be at a height sufficient to slightly look down at the tops of the solar modules.

Second, since the panels will be mounted on single axis tracking systems, the surface of the panels will always try to follow the position of the sun (but fixed in one axis). Due to this property, steep glancing angles are minimized as compared to a non-tracking system.

Lastly, glare is avoided when vegetation or other impediments are located between the observer and the solar modules. A home, for example, may be in the general area of a site with solar PV modules. That house, however, is at no risk of exposure to solar glare if other buildings or trees stand between it and the solar modules.

1.3 Overview of Sun Movements and Relative Reflections

The basic concept to understand in any discussion of glare elevation is that the angle of incidence is always equal to the angle of reflectance. The empirical inquiry is then whether the potential observer is within the altitude of reflection given the distance of the observer from the solar PV panel. At any angle of reflectance, as a potential observer is further and further away from the solar PV panel, the elevation of the reflected sunlight (i.e., any glare) is more likely to be above the observer and, thus, not seen. In contrast, at a high angle of reflectance, the elevation of reflected sunlight will likely be above the observer-even at short distances.

Given the basic principle of light reflectivity, evaluating the angle of reflectance from a solar PV panel must begin with a determination of the altitude of the sun (in degrees) relative to the ground. The "solar altitude" is the angle of the sun in degrees above or below the horizon. As such, the most important consideration when calculating light reflectivity is not the horizon, but the angle at which the solar panel is mounted relative to the horizon.

As the angle of the sun in relation to the solar PV panel increases, the angle of reflection will decrease, and the altitude of reflection will increase. The altitude of the sun differs based on several different factors: the time of day, the season of the year, and the latitude at which the solar PV panel is located.

1.3.1 Determining the Vector Location of Incident Sunlight

The sun's apparent path across the sky changes slightly every day in known and predictable ways depending on the location of the subject area on the earth and date of the year. At any given instant, the sun's position in the sky can be described by a directional vector characterized by an azimuth and an elevation. An azimuth is defined as the angle of the sun's position from due north in a clockwise direction. For example, if the sun rose exactly in the east and set exactly in the west, the azimuth of the sunrise would be 90° from north, and the sunset would occur at 270° from the north. The sun's elevation is defined as the degrees of the sun's orb above the horizon at any instant in time. Other azimuth conventions consider azimuth from north to south along the east half as ranging from 0° to 180°, and along the west half as ranging from 0° to -180°.

Sun path chart diagrams plot the azimuth and elevation of the sun at any instant in time for any location on the earth. A sun path chart for the latitude and longitude of the proposed Project is shown in **Figure 5**.

As depicted in **Figure 5**, the sun's path for a given date is shown in blue and the time during which the sun is at a specific location in the sky is shown in red. For the location of a given receptor such as an air-traffic control facility, the solar elevation and azimuth where reflections would be received at the receptor can be calculated and plotted on the solar chart. For example, for the hypothetical receptor shown in green, reflected light would only be received when the sun is between approximately 75° and 90° azimuth (from north) and at an elevation between 22° and 40°. From the chart, this would occur between 8 and 9 a.m. between the dates of March 20 to April 20.

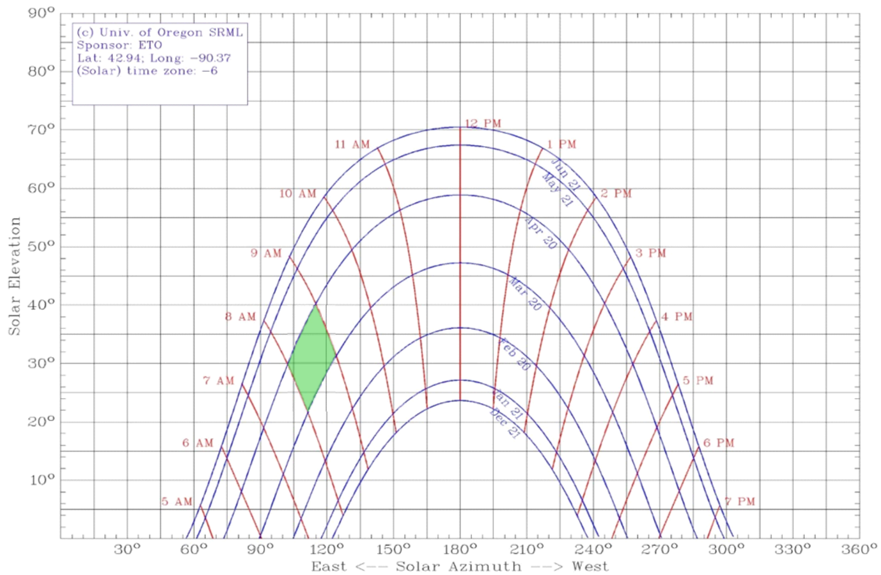

Figure 5: Solar Path Chart Plotting Solar Azimuths and Elevations as a Function of Time and Date for the Location of the Proposed Solar Project

1.3.1 Sunlight Geometry

The determination and characterization of the geometry of incident and reflected light is a mathematical process that is based on angles and vectors in three-dimensional coordinate systems. Light reflected from a surface is described in **Figure 6a** and shows that reflected light is symmetrical about the normal of the surface. All methods used to calculate the path of reflected rays assume this symmetric condition.

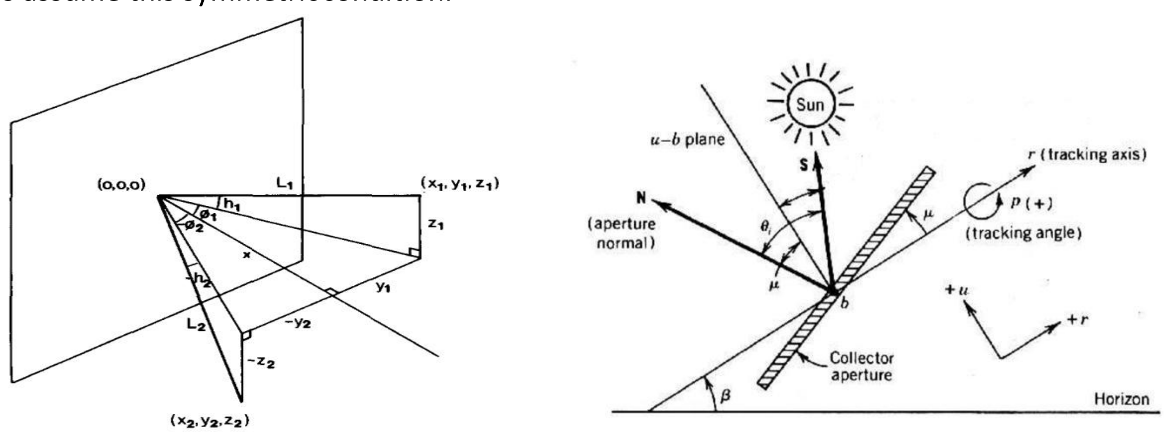

(a) (b)

Figure 6: (a) Geometry of the Reflection (L2) of an Incident Ray of Sunlight (L1) from a Vertical Reflective Surface (Source: Lillefair 1987). (b) Reflections from a Sloping Reflective 1-Single Axis Tracker Surface. (Source: Stine and Geyer 2001)

2.0 DESCRIPTION OF THE PROPOSED PROJECT

The Project may use PV modules from a variety of manufacturers. The modules will be divided in ranks and arranged in a series of irregular rectangular units. Modules will likely be stacked one or two modules high (portrait configuration) on a single-axis tracker system (**Figure 7**). The tracker will rotate east to west along a north-south axis from the horizontal in east-west oriented ranks with the panel normal oriented due south (**Figures 8** and **9**). When installed, the module height aboveground will range from 2 ft. at their lowest point to up to 15 ft. at the highest point (**Figure 10**). In the analysis an average height of 6 ft. was used.

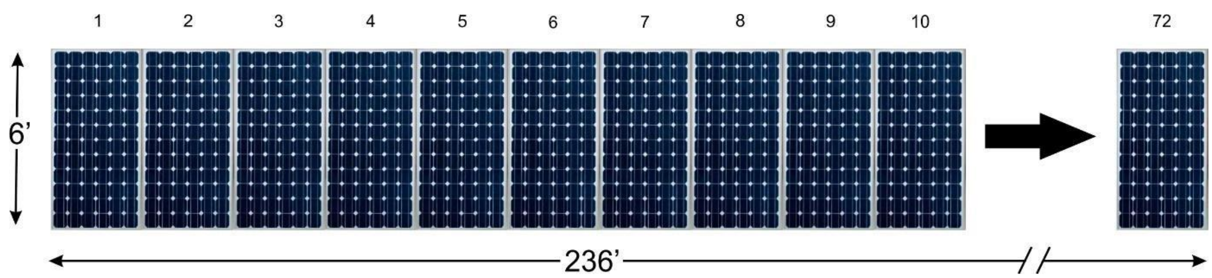

Figure 7: Diagram of the Racking System Configuration for the Proposed Project

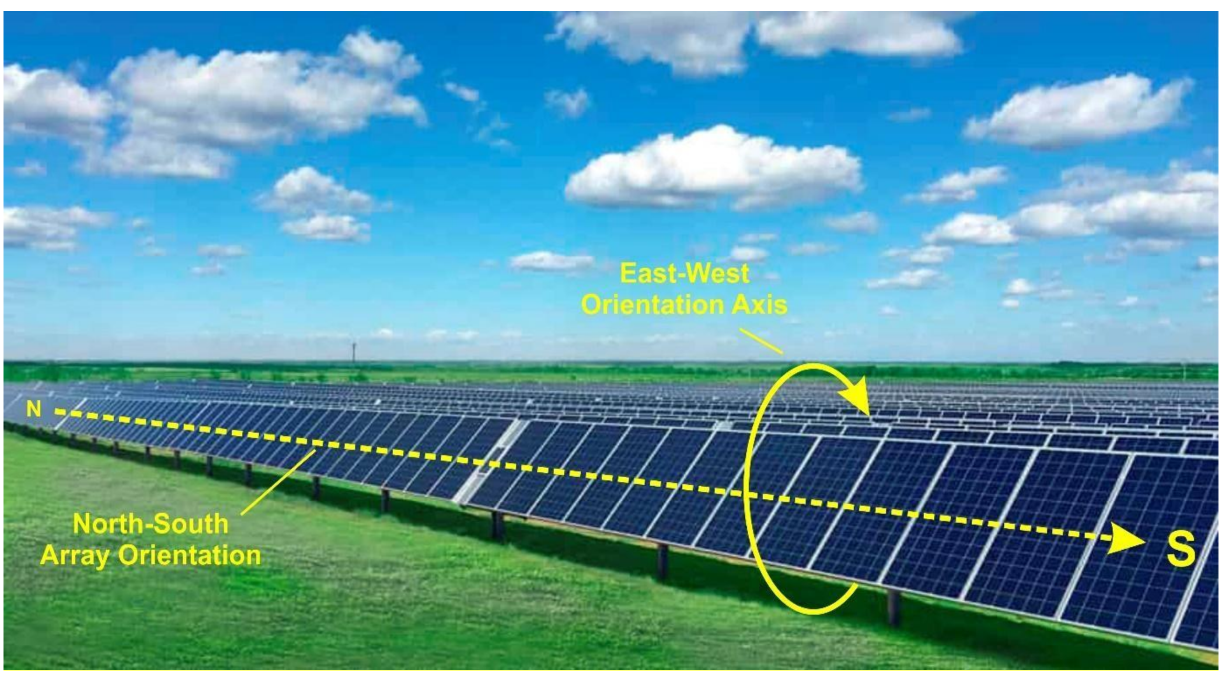

Figure 8: Diagram Showing Tracker Array Rotation and Orientation for the Proposed Project

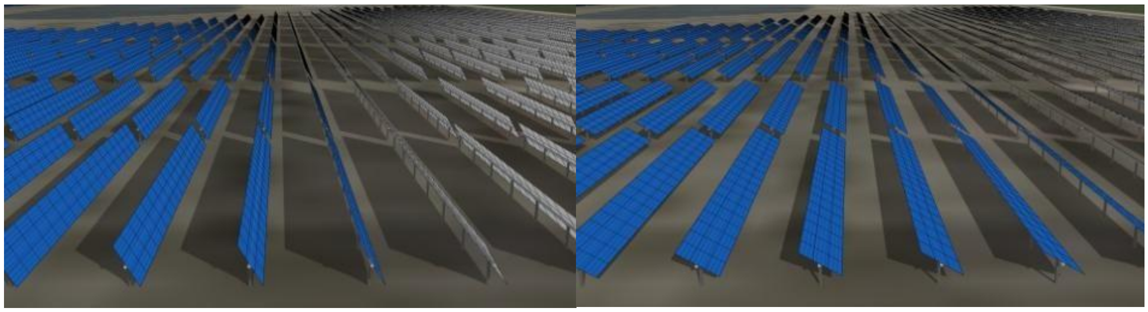

(a) (b)

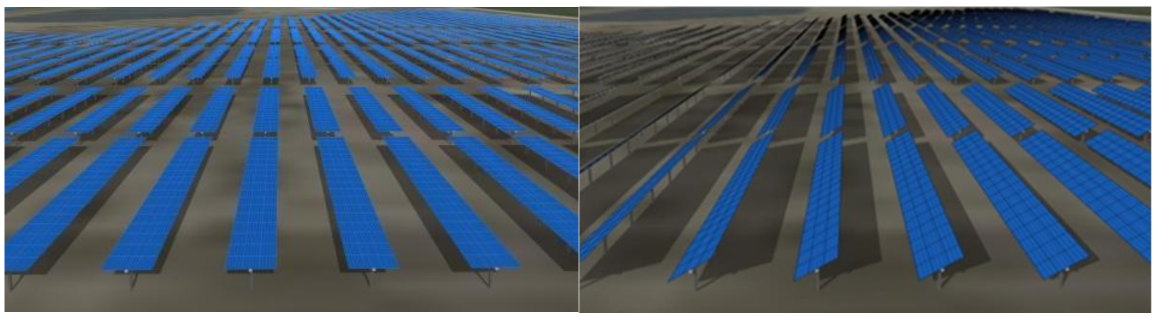

(c) (d)

Figure 9: Solar PV Tracker System Configuration at (a) 9:00 AM, (b) 10:00 AM, (c) 12:00 PM, and (d) 2:00 PM on December 21st, the Winter Solstice

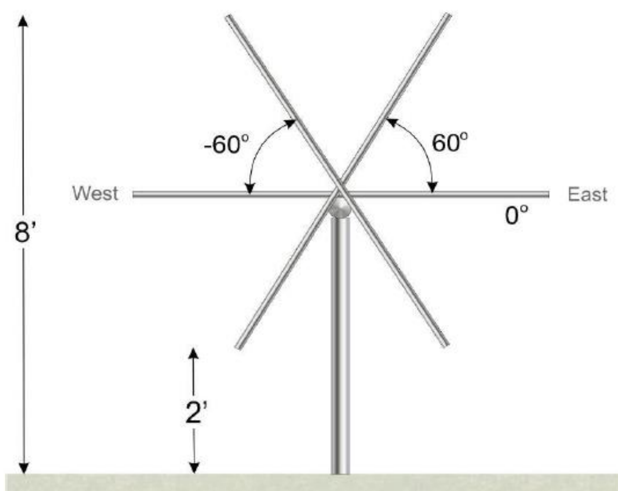

Figure 10: Typical 1-Axis Tracking System Configuration (modules are approximately 2 feet off the ground at their extreme tilt of ±60°)

2.1 Geometric Characteristics of Photovoltaic Panel Configuration and Their Influence on Perceived Glint and Glare

With respect to assessing the impacts of reflected sunlight associated with PV modules for the proposed Project, the following assumptions apply:

1. Perceived glint and glare were based on line-of-sight from the reflective surface without accounting for visual screening from vegetation or buildings.

2. The magnitude and duration of glint and glare reflections will be related to the height of the observer. When the height of the observer is less than the module height and the landscape is flat, only one reflecting rank of PV modules will be visible at a time.

3. Stationary receptors that are below the top height of the PV modules will only see glint and glare from those modules whose reflective surfaces are visible from that location. The glint and glare will move as the sun moves until the azimuth and elevation of the sun's rays are such that reflections are no longer received at the stationary receptor.

4. Because the orientation of each rank is the same, each rank will reflect glint and glare at the same angle for the same time increment and given azimuth and elevation angle of the sun. Thus, if a plane with the observer at a height below the highest point of the PV rank observes a solar reflection, the same reflection at the same relative location will be observed as the plane proceeds parallel to the PV ranks.

5. As the height of the stationary receptor increases above the height of the PV rank, progressively more of the area of adjacent ranks will be observed. At low heights, most of the PV panel area of successive ranks is blocked, but as heights increase progressively more of the reflective area of the full array becomes contributing.

3.0 IDENTIFICATION OF FLIGHT PATHS

Four flight paths (FPs) were modeled for potential glare impacts. These FPs extend from the runway to 2 miles from the end of the Faribault Airport runways. The FP1 is directed at 300°; FP2 directed at 120°; FP3 is directed at 10°; and FP4 is directed at 190°. The flight paths were modeled with a threshold height of 50 feet AGL at the end of the runway with a 3-degree glide slope was used to simulate an average eye level for pilots (**Table 1**). The locations of the flight paths were determined from an examination of runways within the vicinity of the Project that could be subjected to glare (**Table 2**).

Table 1. 2-Mile Flight Path Receptor Points 1-4

	Point	Latitude (°)	Longitude (°)	Ground elevation (ft)	Height above ground (ft)	Total elevation (ft)
1	Threshold	44.324827	-93.305858	1047.75	50.00	1097.75
	Two-mile	44.306840	-93.274178	961.35	689.83	1651.18
2	Threshold	44.331092	-93.317466	1058.55	50.00	1108.55
	Two-mile	44.348617	-93.349652	1055.65	606.33	1661.98
3	Threshold	44.327730	-93.316517	1048.75	50.00	1098.75
	Two-mile	44.299256	-93.323544	982.87	669.34	1652.21
4	Threshold	44.333801	-93.315047	1054.07	50.00	1104.07
	Two-mile	44.362275	-93.308020	1050.61	606.92	1657.52

FARIBAULT MUNI–LIZ WALL STROHFUS FLD (FBL)(KFBL) 3 NW UTC–6(–5DT) N44°19.74´ W93°18.78´ **OMAHA L–12J IAP**

1060 B NOTAM FILE FBL

RWY 12–30: H4257X75 (ASPH) S–16, D–22 MIRL 0.3% up NW

RWY 12: REIL. PAPI(P4L)—GA 3.0° TCH 40´. Tree.

RWY 30: REIL. PAPI(P4L)—GA 3.0° TCH 40´. Thld dsplcd 230´. Road.

RWY 01–19: 2300X175 (TURF)

RWY 01: Crops.

RWY 19: Tree.

SERVICE: S4 **FUEL** 100LL, JET A **OX** 4 **LGT** MIRL Rwy 12–30 preset to low, to incr ints and ACTIVATE REIL Rwy 12 and Rwy 30—CTAF. Rwy 12 PAPI ops continuously. Rwy 30 PAPI opr continuously.

AIRPORT REMARKS: Attended May–Sep 1400–0000Z‡, Oct–Apr Mon–Fri 1400–0000Z‡, Oct–Apr Sat 1600–2100Z‡, Oct–Apr Sun unattended. For svc after hrs call 507–838–7152. Self svc fuel with credit card. Rwy 01–19 not plowed winter months. Open for skiplanes. When landing on Rwy 12, be alert for turbulence and possible windshear when winds are out of the south. Ultralights and gliders use twy and extended twy parallel to Rwy 12–30. Ultralights and gliders using twy fly pattern on NE side of Rwy 12–30. Rwy 01–19 marked with yellow cones.

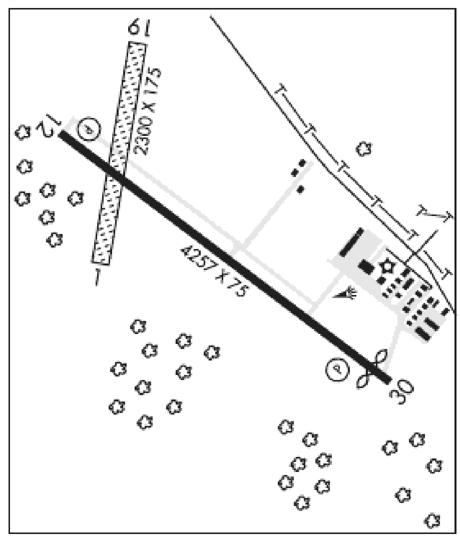

AIRPORT MANAGER: 507-332-0140

WEATHER DATA SOURCES: AWOS–3 120.2 (507) 332–2505.

COMMUNICATIONS: CTAF/UNICOM 122.8

Ⓡ **MINNEAPOLIS APP/DEP CON** 134.7

GCO 121.725 (MINNEAPOLIS CLNC and FLIGHT SERVICES)

CLEARANCE DELIVERY PHONE: For CD ctc Minneapolis Apch at 612-726-9086.

RADIO AIDS TO NAVIGATION: NOTAM FILE PNM.

HALFWAY (T) VORW/DME 111.2 FOW Chan 49 N44°12.27´ W93°22.23´ 016° 7.9 NM to fld. 1100/2E.

VOR/DME unmonitored.

VOR portion unusable:

230°–250°

VFRMAP.COM APR-2021

Table 2 Faribault Municipal Airport

4.0 GLINT AND GLARE ASSESSMENT METHODOLOGY

For modeling purposes, the Project was put into a PV array area as shown in **Exhibit 2**. To model the potential intensity and time of project-related glare to receptors, Westwood used the ForgeSolar GlareGauge solar glare analysis software (formally the Solar Glare Hazard Analysis Tool

[SGHAT]). GlareGauge is a web-based tool that estimates when and where solar glare could occur throughout a typical year from a PV array as viewed from specified observer locations. GlareGauge uses an interactive ArcMap or Google Maps interface together with a few user-specified parameters such as orientation and tilt of the modules to quickly locate a site, outline the proposed array, and calculate the occurrence, intensity, and size of the potential glare throughout the year.

If glare potential is predicted, the GlareGauge calculates the retinal irradiance and subtended angle (size/distance) of the glare source to estimate potential ocular hazards. Ocular hazards range in severity from a potential temporary after-image to retinal burn. GlareGauge produces a color-coded display of the potential for glare to result in an ocular impact. The classifications are low potential for producing an after-image (green), potential for producing an after image (yellow), and potential for permanent eye damage (red).

After the project area is determined and its design characteristics are known, information from each glare-sensitive receptor is input into the model. Each of the FP's were identified on the project map and the height of the observer was incorporated. Each FP was assessed with a 10-degree solar panel resting angle. An example of the GlareGauge model is described in **Table 3**.

PV Array Parameters Example

Table 3: Example of PV Panel Input Parameters for 6 feet and 10 Degree Resting Angles

Name: A10
Axis tracking: Single-axis rotation
Tracking axis orientation: 180.0°
Tracking axis tilt: 0.0°
Tracking axis panel offset: 0.0°
Max tracking angle: 60.0°
Resting angle: 10.0°
Rated power: -
Panel material: Light textured glass with AR coating
Reflectivity: Vary with sun
Slope error: correlate with material

Vertex	Latitude (°)	Longitude (°)	Ground elevation (ft)	Height above ground (ft)	Total elevation (ft)
1	44.322078	-93.314027	1044.65	6.00	1050.65
2	44.321800	-93.314030	1043.75	6.00	1049.75
3	44.321796	-93.313339	1044.05	6.00	1050.05
4	44.320041	-93.313359	1037.85	6.00	1043.85
5	44.320044	-93.313964	1038.75	6.00	1044.75
6	44.319767	-93.313967	1036.65	6.00	1042.65
7	44.319771	-93.314601	1037.55	6.00	1043.55
8	44.322081	-93.314574	1039.05	6.00	1045.05

<u>*Tilt of Tracking Axis*</u> – Elevation angle of the tracking axis in degrees, where 0° is facing skyward and 90° is facing horizontally. The modules rotate about the tracking axis. 0° was selected as the modules will be facing up.

<u>*Orientation of Tracking Axis*</u> – Orientation of the tracking axis in degrees, measured clockwise from true north. In this case the value was determined to be 180°.

<u>*Offset angle of Module*</u> – The vertical offset angle between the tracking axis and the panel. No offset

was selected for the single axis tracker.

Maximum tracking angle – The maximum angle the panel will rotate in both the clockwise and counterclockwise directions from the zenith (upward) position. The maximum rotation limit currently under consideration is ±60^0.

Rated Power (kW) – kW power of solar PV plant. No rated power was selected for the proposed size of the solar arrays because the area of panel coverage is the primary factor at this site.

Module Surface Material – Type of PV material used and surface finish of panel. According to specifications from the module manufacturers, it was determined that the input 'Smooth Glass with ARC" would be the most representative option.

Reflectivity of PV module – The near-normal specular reflectance of PV glass (e.g., with ARC) can be as low as 2%, the reflectance can increase as the incidence angle of the sunlight increases (glancing angles). This number is based in part on the array parameters shown in **Table 2**.

Slope error – Mirror-like surfaces that produce specular reflections will have a slope error closer to zero, while rough surfaces that produce more scattered (diffuse) reflections have higher slope errors. Based on typical values for the module types under consideration, a value of 8.43 mrad was used.

Latitude and Longitude – The latitude and longitude of the PV array boundary vertices were used to define the area covered by proposed PV array. Appendix A provides the coordinates of the perimeter and their map image which also correspond to PV arrays shown in **Exhibit 2**. GlareGauge creates a reflective plane using elevation values of the array for the glint and glare assessment.

Ground Elevation – Elevation of vertices above sea level. Values are input into the table once the vertex is located. This is considered the point's base elevation. This value is used to shape the reflective plane used to estimate glint and glare.

Height above Ground – User input to modify/correct vertex elevation above ground. This is defined as 'PV array installation height above ground'. Since this Project will use a single axis tracker system an average value of 6 feet was used. Actual height varies from 2 to 14 feet above ground (see **Figure 10**).

Total Elevation – Calculated after adding the '*Ground Elevation*' and "*Height above Ground*'. All units are in feet.

OP Parameters

OP parameters were calculated using GIS software and aerial photographs of the Project. Location, elevation, and a calculated field of the receptors were used. A 5-foot height above ground was used for first floor receptor height. A 15-foot height above ground was used for second floor receptor height. These parameter units are in feet. Please note that OPs were not used for this Project.

FP Parameters
FP parameters were calculated using GIS software and aerial photographs of the Project. Location, elevation, and a calculated field of receptors were used. A 50-foot threshold height and 3-degree glide path above ground was used for receptor height. These parameter units are in feet (**Appendix A**).

Total Elevation – Is calculated after adding the '*Ground Elevation*' and '*Height above Ground*'. All units are in feet.

Ground Elevation – Elevation of FPs above sea level. Values are pulled into the table once the FP is located. This is the point's base elevation.

Eye level Height above ground – User input to modify/correct observer's elevation above ground.

5.0 GLINT AND GLARE RESULTS

5.1 Flight Paths (FPs)

Results from the GlareGauge analysis determined that no glint or glare (green, yellow, or red) would be visible at the four FPs with a 10-degree resting angle and that the assessment passed the Forge Solar FAA policy adherence as shown in **Appendix A**.

6.0 REFERENCES

Capital Solar Farm Visual Impact Assessment (2010): Available at https://majorprojects.affinitylive.com/public/a56f5113529f7061acb6de0cb400a52e/Capital%20EA%20Final%201.0%20Appendix%20F_compressed-_Part4%20.pdf

Littlefair, P.D. 1987. Prediction of reflected solar dazzle from sloping facades. Building and environment 22(4):285-291).

Sandia National Laboratories (Sandia). 2014. Solar Glare Hazard Analysis Tool (SGHAT) User's Manual, Ver 2D. Sandia National Laboratories. 34 pp.

Stine, W.B. and M. Geyer. 2001. Power from the Sun. e-book Power from the Sun.net.

7.0 RESUMES

Westwood

THOMAS BRAMAN
Senior Environmental Scientist

Overview

Tom currently is a Senior Environmental Scientist at Westwood. He has over 30-years of experience and completed nearly 2,000 projects. He works on solar and wind renewable power projects but also electrical transmission, oil, gas, and pipeline, transportation, communication, commercial and residential developments. Tom's has an undergraduate education in biology and photography and graduate studies in agricultural economics. He also has years of agricultural production experience as a commercial vegetable grower.

Tom has worked on over 400 solar projects across the United States He has completed work for solar clients in AZ, CA, CO, IA, IL, IN, KY, LA, MI, MN, MO, ND, NJ, NY, OH, TX, VA, WV, and WI. He has completed glare studies on projects ranging from 1MW to over 600 MW across the country.

Elliott Solar, IN
Glare analysis modeling for the proposed 200MW solar in Gibson Co. Prepared for Confidential Client.

Gerdeau Solar, TX
Glare analysis and alternative design assessment modeling for the proposed solar project adjacent to a neighborhood and highway in Gerdau, TX area. Prepared for Confidential Client

Koshkonong Solar, WI
Glare analysis modeling, alternative design assessments for the proposed solar project in Dane Co., WI, Prepared for Confidential Client.

Paris, Darien and Badger Hollow Solar, WI
Glare analysis modeling for alternatives associated with the three proposed 100+ MW solar projects adjacent to residences, businesses, and airport in these areas.

Thomas Hill Solar, MO
Glare analysis modeling, alternative design assessments for the proposed solar 1,000-acre project in Randolph Co., Prepared for Confidential Client.

Exhibits

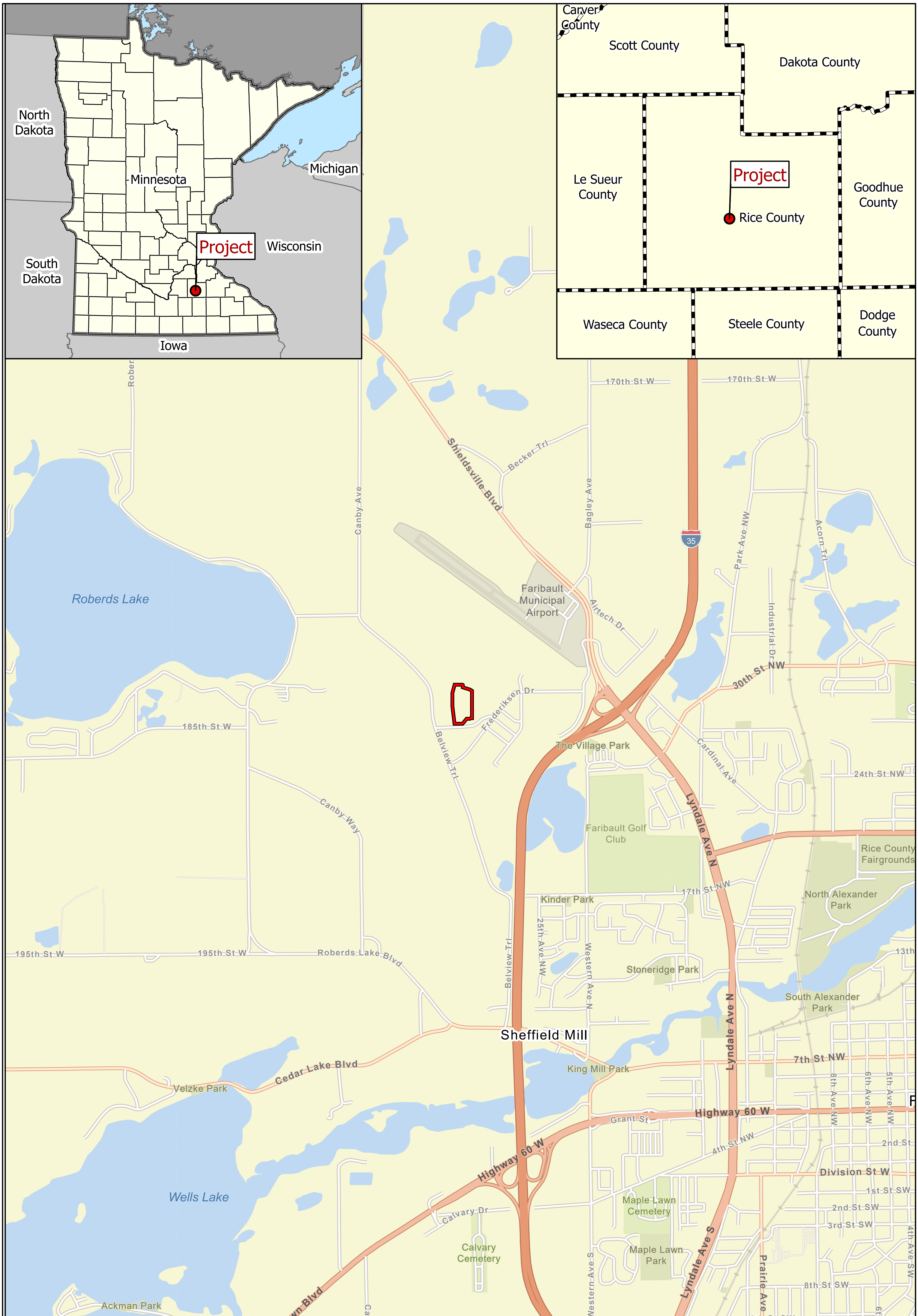

Data Source(s): Westwood (2021); ESRI WMS World Streets Basemap; U.S. Census (2008).

Legend

- Solar Array Fence
- County Boundary
- State Boundary

N

0 2,100 Feet

Fair Park Solar Project

Rice County, Minnesota

Site Location

Exhibit 1

Westwood

Toll Free (888) 937-5150 westwoodps.com

Westwood Professional Services, Inc.

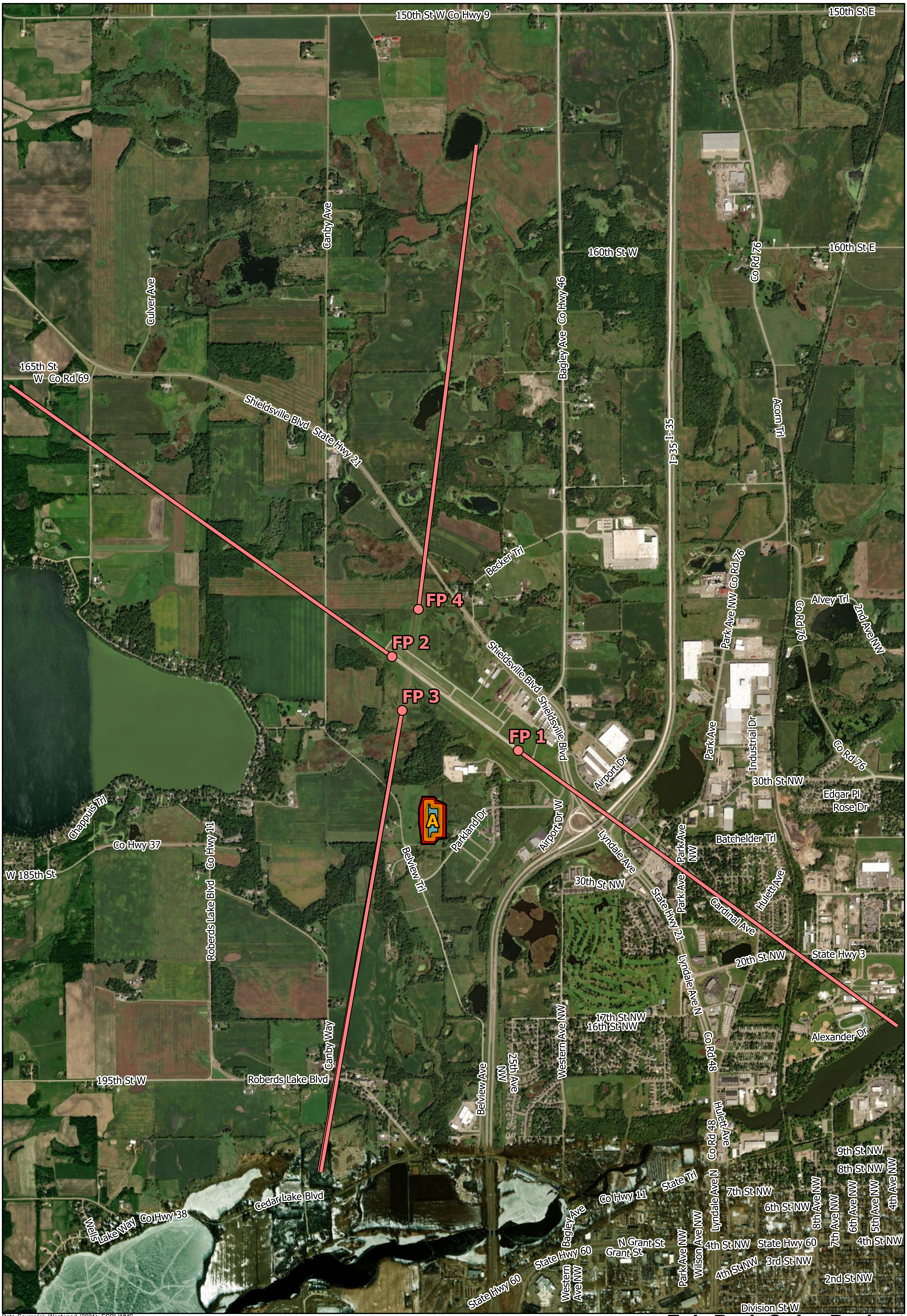

Data Source(s): Westwood (2021); ESRI WMS Imagery Basemap; U.S. Census (2019).

Legend

- Solar Array Fence
- Solar Array Group
- Flight Path (FP)

N

0 2,000 Feet

Fair Park Solar Project

Rice County, Minnesota

Glare Study Overview

Exhibit 2

Westwood

Toll Free (888) 937-5150 westwoodps.com

Westwood Professional Services, Inc.

Appendix A

FORGESOLAR GLARE ANALYSIS

Project: **Fairpark**
Site configuration: **Array 1_10 DRA_4FP**
Analysis conducted by Tom Braman (Tom.Braman@westwoodps.com) at 20:29 on 17 Jun, 2021.

U.S. FAA 2013 Policy Adherence

The following table summarizes the policy adherence of the glare analysis based on the 2013 U.S. Federal Aviation Administration Interim Policy 78 FR 63276. This policy requires the following criteria be met for solar energy systems on airport property:

- No "yellow" glare (potential for after-image) for any flight path from threshold to 2 miles
- No glare of any kind for Air Traffic Control Tower(s) ("ATCT") at cab height.
- Default analysis and observer characteristics (see list below)

ForgeSolar does not represent or speak officially for the FAA and cannot approve or deny projects. Results are informational only.

COMPONENT	STATUS	DESCRIPTION
Analysis parameters	PASS	Analysis time interval and eye characteristics used are acceptable
2-mile flight path(s)	PASS	Flight path receptor(s) do not receive yellow glare
ATCT(s)	N/A	No ATCT receptors designated

Default glare analysis parameters and observer eye characteristics (for reference only):

- Analysis time interval: 1 minute
- Ocular transmission coefficient: 0.5
- Pupil diameter: 0.002 meters
- Eye focal length: 0.017 meters
- Sun subtended angle: 9.3 milliradians

FAA Policy 78 FR 63276 can be read at https://www.federalregister.gov/d/2013-24729

SITE CONFIGURATION

Analysis Parameters

DNI: peaks at 1,000.0 W/m^2
Time interval: 1 min
Ocular transmission coefficient: 0.5
Pupil diameter: 0.002 m
Eye focal length: 0.017 m
Sun subtended angle: 9.3 mrad
Site Config ID: 54761.9835

PV Array(s)

Name: A10
Axis tracking: Single-axis rotation
Tracking axis orientation: 180.0°
Tracking axis tilt: 0.0°
Tracking axis panel offset: 0.0°
Max tracking angle: 60.0°
Resting angle: 10.0°
Rated power: -
Panel material: Light textured glass with AR coating
Reflectivity: Vary with sun
Slope error: correlate with material

Vertex	Latitude (°)	Longitude (°)	Ground elevation (ft)	Height above ground (ft)	Total elevation (ft)
1	44.322078	-93.314027	1044.65	6.00	1050.65
2	44.321800	-93.314030	1043.75	6.00	1049.75
3	44.321796	-93.313339	1044.05	6.00	1050.05
4	44.320041	-93.313359	1037.85	6.00	1043.85
5	44.320044	-93.313964	1038.75	6.00	1044.75
6	44.319767	-93.313967	1036.65	6.00	1042.65
7	44.319771	-93.314601	1037.55	6.00	1043.55
8	44.322081	-93.314574	1039.05	6.00	1045.05

Flight Path Receptor(s)

Name: FP 1
Description: None
Threshold height: 50 ft
Direction: 300.0°
Glide slope: 3.0°
Pilot view restricted? Yes
Vertical view: 30.0°
Azimuthal view: 50.0°

Point	Latitude (°)	Longitude (°)	Ground elevation (ft)	Height above ground (ft)	Total elevation (ft)
Threshold	44.324827	-93.305858	1047.75	50.00	1097.75
Two-mile	44.306840	-93.274178	961.35	689.83	1651.18

Name: FP 2
Description: None
Threshold height: 50 ft
Direction: 120.0°
Glide slope: 3.0°
Pilot view restricted? Yes
Vertical view: 30.0°
Azimuthal view: 50.0°

Point	Latitude (°)	Longitude (°)	Ground elevation (ft)	Height above ground (ft)	Total elevation (ft)
Threshold	44.331092	-93.317466	1058.55	50.00	1108.55
Two-mile	44.348617	-93.349652	1055.65	606.33	1661.98

Name: FP 3
Description:
Threshold height: 50 ft
Direction: 10.0°
Glide slope: 3.0°
Pilot view restricted? Yes
Vertical view: 30.0°
Azimuthal view: 50.0°

Point	Latitude (°)	Longitude (°)	Ground elevation (ft)	Height above ground (ft)	Total elevation (ft)
Threshold	44.327730	-93.316517	1048.75	50.00	1098.75
Two-mile	44.299256	-93.323544	982.87	669.34	1652.21

Name: FP 4
Description:
Threshold height: 50 ft
Direction: 190.0°
Glide slope: 3.0°
Pilot view restricted? Yes
Vertical view: 30.0°
Azimuthal view: 50.0°

Point	Latitude (°)	Longitude (°)	Ground elevation (ft)	Height above ground (ft)	Total elevation (ft)
Threshold	44.333801	-93.315047	1054.07	50.00	1104.07
Two-mile	44.362275	-93.308020	1050.61	606.92	1657.52

GLARE ANALYSIS RESULTS

Summary of Glare

PV Array Name	Tilt (°)	Orient (°)	"Green" Glare min	"Yellow" Glare min	Energy kWh
A10	SA tracking	SA tracking	0	0	-

Total annual glare received by each receptor

Receptor	Annual Green Glare (min)	Annual Yellow Glare (min)
FP 1	0	0
FP 2	0	0
FP 3	0	0
FP 4	0	0

Results for: A10

Receptor	Green Glare (min)	Yellow Glare (min)
FP 1	0	0

Receptor	Green Glare (min)	Yellow Glare (min)
FP 2	0	0
FP 3	0	0
FP 4	0	0

Flight Path: FP 1

0 minutes of yellow glare
0 minutes of green glare

Flight Path: FP 2

0 minutes of yellow glare
0 minutes of green glare

Flight Path: FP 3

0 minutes of yellow glare
0 minutes of green glare

Flight Path: FP 4

0 minutes of yellow glare
0 minutes of green glare

Assumptions

"Green" glare is glare with low potential to cause an after-image (flash blindness) when observed prior to a typical blink response time.
"Yellow" glare is glare with potential to cause an after-image (flash blindness) when observed prior to a typical blink response time.
Times associated with glare are denoted in Standard time. For Daylight Savings, add one hour.
Glare analyses do not account for physical obstructions between reflectors and receptors. This includes buildings, tree cover and geographic obstructions.
Several calculations utilize the PV array centroid, rather than the actual glare spot location, due to algorithm limitations. This may affect results for large PV footprints. Additional analyses of array sub-sections can provide additional information on expected glare.
The subtended source angle (glare spot size) is constrained by the PV array footprint size. Partitioning large arrays into smaller sections will reduce the maximum potential subtended angle, potentially impacting results if actual glare spots are larger than the sub-array size. Additional analyses of the combined area of adjacent sub-arrays can provide more information on potential glare hazards. (See previous point on related limitations.)
Glare locations displayed on receptor plots are approximate. Actual glare-spot locations may differ.
Glare vector plots are simplified representations of analysis data. Actual glare emanations and results may differ.
The glare hazard determination relies on several approximations including observer eye characteristics, angle of view, and typical blink response time. Actual results and glare occurrence may differ.
Hazard zone boundaries shown in the Glare Hazard plot are an approximation and visual aid based on aggregated research data. Actual ocular impact outcomes encompass a continuous, not discrete, spectrum.
Refer to the Help page at **www.forgesolar.com/help/** for assumptions and limitations not listed here.